http://dx.doi.org/10.5012/bkcs.2014.35.8.2251

Easy Preparation of Nanosilver-Decorated Graphene Using Silver Carbamate by Microwave Irradiation and Their Properties

Sang-Woo Yun, Jae-Ryung Cha, and Myoung-Seon Gong*

*Department of Nanobiomedical Science & BK21 PLUS NBM Global Research Center for Regenerative Midicine, Dankook University Graduate School, Cheonan, Chungnam 330-714, Korea. *E-mail: msgong@dankook.ac.kr*
Received March 12, 2014, Accepted April 3, 2014

We have successfully decorated reduced graphene oxide (RGO) with silver nanoparticles (AgNPs) by microwaving silver alkylcarbamate for 13 seconds using 1-amino-4-methylpiperazine. Uniform AgNPs (20–40 nm) were effectively prepared, and 1-amino-4-methylpiperazine acted as a reaction medium, reducing agent, and stabilizer. Particle size and morphology were correlated with the silver alkylcarbamate concentration and microwave time. The graphene/AgNPs composites were characterized by Raman, X-ray diffraction, and scanning electron microscopy to confirm that the AgNPs were uniformly decorated onto the graphene. Measurements of the transparent conductive property at room temperature indicated that these graphene/AgNPs nanosheets with 55.45% transmittance were electrically continuous with a sheet resistance of approximately 43 kΩ/□.

Key Words : Silver nanoparticles, 1-Amino-4-methylpiperazine, Silver alkylcarbamate, Microwave, Graphene/Ag-NPs composites

Introduction

Graphene is a monolayer of carbon atoms that are tightly packed into a two-dimensional, honeycomb crystal structure.[1] This extremely thin nanomaterial has shown fascinating properties and holds promise for future carbon based device architecture, due to high mechanical stiffness, extraordinary electronic transport properties, and excellent antibacterial activity.[2-4]

Graphene oxide (GO) is strongly hydrophilic and can generate a stable and homogeneous colloidal suspension in aqueous and various polar organic solvents due to the negatively charged GO sheets.[3,5] Subsequent deoxygenation *via* chemical reduction removes most of the oxygen-containing groups and the obtained bulk graphene sheets restack to form graphite if left unprotected.[5,6] Thus, keeping the graphene sheets individually separated is the most important and challenging part of graphene production. Aggregation can be reduced by attaching other molecules or polymers onto the sheets.[6-9] However, the presence of foreign stabilizers is undesirable for some applications, particularly in electronic devices. Only partial restoration of the graphitic structure can be accomplished by chemically reducing the chemically converted graphene, which leads to high sheet resistance.[10] The existence of an insulate dispersant further deteriorates electroconductibility.

In this respect, GO sheets are generally used as the raw material or precursors to graphene sheets due to their good dispersibility in organic solvents. However, the reported protocols for graphene-metal hybrids are relatively complex and generally require two steps of reduction of the GO material and deposition of metal nanoparticles (NPs). A dispute still exists as to where the GO carboxylic acid groups are located. This problem can possibly be resolved by indirect *in situ* deposition of metal NPs on GO because carboxylic acids are normally the nucleation sites for metal NP formation. Through such a method, some researchers have shown that carboxylic acids are located at the edges of the GO, as the NPs fringe the GO/reduced graphene oxide sheets.[11]

Deposition of inorganic NPs, such as metals onto graphene sheets is supposed to be useful for preventing restacking of the graphene sheets.[12] By selecting the appropriate metal NPs, the deposition strategy not only leads to physical separation of the resulting graphene sheets, but also makes it possible to use these new hybrids in chemical sensors, optical and electronic devices, and for energy storage.[13-15] Thus, we considered that if particles with high electric conductivity were deposited onto graphene sheets that good dispersity would be obtained and good conductivity would also be maintained.

In this study, silver carbamate was selected as a precursor for electrically conducting particle to form graphene/Ag nanocomposites using the microwaving solvothermal method. The graphene/AgNPs composites were characterized by Raman, X-ray diffraction, and scanning electron microscopy to confirm that the AgNPs were uniformly decorated onto the graphene. The transparent and conductive property at various temperature was measured to investigate the dispersity and electroconductibility of resulting composites by the microwave assisted solvothermal reaction.

Experimental

Raw Materials. 1-Amino-4-methylpiperazine (AMP) was obtained from commercial sources (Sigma-Aldrich Chem.

Co., St. Louis, MO, USA) and was used without further purification. Graphite powder with an average particle size of 45 μm was purchased from Samjung C&G (Seoul, Korea). Graphite oxide was synthesized *via* the oxidative treatment of natural graphite using the modified Hummer's method.[16] Reduced graphene oxide (RGO) was prepared by reduction of graphene oxide with hydrazine.[17] In this study, the obtained RGO was called graphene. An isopropyl alcohol solution of silver 2-ethylhexyl-ammonium carbamate was purchased from InkTec Co., Ltd. (Korea).

Characterization. X-ray diffraction (XRD) patterns were recorded with a RIGAKU Ultima IV (Japan) powder diffractometer with CuKα radiation (λ = 1.5406 Å) operating at 40 kV and 40 mA. Scanning electron microscopy (SEM; TESCAN MIRA LMH, Czech) was used to observe sample morphology. Fourier transform infrared (FT-IR) spectra were recorded with an Agilent Technologies 640-IR (Palo Alto, CA, USA) FT-IR spectrometer. Raman spectra were recorded with a Horiba Jobin-Yvon T-64000 (Tokyo, Japan) Raman spectrometer; the excitation line at 632.8 nm provided by an Ar+ laser was used. UV-visible spectra were recorded in the range of 200–800 nm using a Cary 100 instrument (Agilent Technologies). The graphene/AgNP suspension was diluted 10 times to record the UV-visible spectra. Sheet resistance was measured with a four point probe (AIT Co., Ltd., CMT-2000N, Seoul, Korea). Transparencies were recorded by a UV-visible spectrophotometer (UV-1601, Shimadzu, Tokyo, Japan).

Preparation of Graphene/AgNPs Nanocomposites in AMP using Microwave Reduction. The graphene/AgNPs were prepared in a one-step reaction. In a typical procedure, graphene powder (10 mg) was added to a solution of silver 2-ethylhexylammonium carbamate (0.1 g, 10 wt % in isopropanol) dissolved in dry AMP (6 mL) in a vial. The vial was exposed to ultrasound to disperse the reaction mixture. The reaction mixtures were allowed to irradiate in a microwave oven for 3, 7, and 13 seconds. Finally, the precipitates were centrifuged (8,000 rpm for 15 min) to produce the graphene/AgNPs. The resulting composites were dried under vacuum at 60 °C for 12 h. Table 1 lists the synthetic conditions.

Deposition of Graphene/AgNPs Coating on a Polymer Film. The graphene/AgNPs (100 mg) were dispersed in a solution of *n*-octyl thioglycolate (100 mg) in isopropanol (50 mL) by sonication for 10 min. The thiol-treated graphene/AgNPs were centrifuged and washed with methanol several times. The washed powder was dried in a vacuum oven at 50 °C for 8 h. The graphene/AgNP coating solution was prepared by dispersing the thiol-treated graphene/Ag-NPs (30 mg) in isopropanol (50 mL). The thin graphene and graphene/AgNPs films were coated using the modified vacuum filtration method.[10] The graphene or graphene/Ag-NPs suspensions were vacuum-filtered using a mixed cellulose ester membrane with 25 nm pores (Millipore, Milford, MA, USA). The graphene and graphene/AgNPs films were allowed to dry and adhere to a PET substrate at room temperature under a 1 kg weight over night. The weight was removed, and the membrane was dissolved using acetone and washed with methanol. Graphene/Ag film was prepared from the solution of graphene (5 mg) dispersed in silver 2-ethylhexyl carbamate (0.5 g) and isopropanol (50 mL) using spin-coating technique (2500 rpm for 2 min).

Results and Discussion

Reducing silver carbamate in AMP using a microwave produced AgNPs with a relatively uniform distribution compared with any other method reported previously.[18,19] However, growth of the AgNPs depended on the microwave time and the silver carbamate concentration. The particle size distribution became slightly broad with an increase in microwave time. AMP was used as a medium in the silver colloidal solution, a reducing agent, and a stabilizer of AgNPs. Therefore, we easily prepared size-controlled graphene/AgNPs composites within 13 seconds without any byproduct contamination due to its versatile role in synthesizing AgNPs. Upon microwaving the AMP solution, it changed from colorless to dark green to brown with a reaction time of 3–13 seconds.

Table 1. Reaction conditions for graphene/AgNPs synthesis

Sample Number	AgEHCB[a] (mg)	AMP[b] (mL)	Graphene (mg)	Reaction time (Sec)
S1	-	-	10	-
S2	5	6	10	7
S3	10			3
S4	10			7
S5	10			13
S6	15			7
S7	20			7
S8	25			7
S9	20			13

[a]silver 2-ethylhexylcarbamate. [b]1-amino-4-methylpiperazine

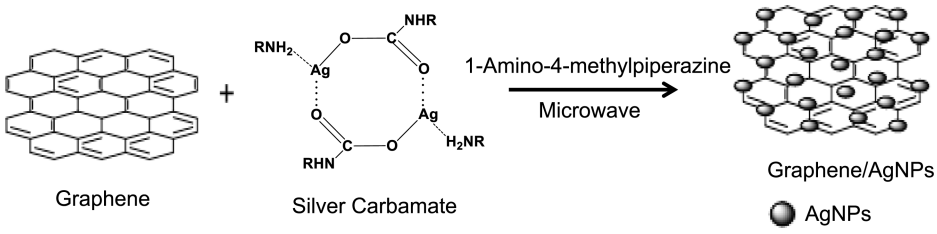

Scheme 1. Schematic diagram showing the preparation of graphene/AgNPs.

Transmission Electron Microscopy (TEM) and SEM Analysis. Figures 1 and 2 show the TEM and SEM images of graphene and graphene/AgNPs with different silver doping dosages. A closely packed lamellar and plate structure and clean surface of graphene is observed (Figure 2(a)). After the graphene was doped with AgNPs, the Ag crystallites were deposited on graphene surfaces as spacers to keep the neighboring sheets separate as shown in Figure 1(b)-(f). The size and shape of the AgNPs was affected by microwave time. When the dosage of silver carbamate was fixed at 10 mg in 6 mL of AMP, the size of the AgNPs increased with increasing microwave time from 3 to 13 seconds, as shown in Figure 1(b)-(d).

The size and shape of the AgNPs were also affected by the dosage of silver carbamate. A low dosage revealed a small size and quantity of AgNPs deposited on the graphene sheets (Figure 1(a)). The AgNPs were well separated from each other and distributed randomly on the graphene sheets as spacers to keep the neighboring sheets separate. Some wrinkles were observed on the surface of the graphene/AgNPs, which may be important for preventing aggregation of graphene and maintaining a high surface area with a particular advantage of attaching AgNPs onto the graphene sheets (Figure 1(b)-(d)). After the dosage of silver carbamate was increased from 10 to 25 mg (Figure 1(e)-(f)), the size of AgNPs increased significantly, and the AgNPs tended to agglomerate.

Figure 2 shows typical SEM images of as-prepared graphene/AgNPs hybrids. As shown in Figure 2(b)-(c), well-dispersed AgNPs were deposited on the graphene and the size range of the AgNPs was 30–50 nm.

Compared to these results, particle size and population increased, indicating the enhanced loading content of deposited Ag. AgNPs, ranging in size from 20 nm to 200 nm, were synthesized using AMP, and the morphology of spherical was controlled by varying the silver carbamate concentration and reaction time, as shown in Figure 2(d)-(e).

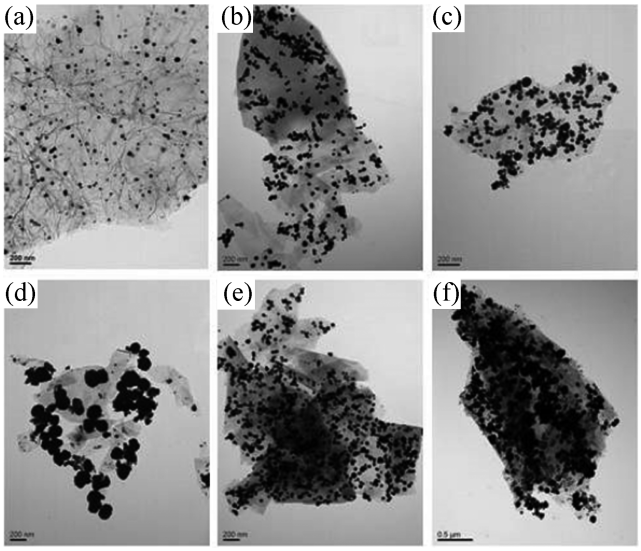

Figure 1. TEM images of graphene/AgNPs (a) S1, (b) S2, (c) S3, (d) S4, (e) S6 and (f) S7 prepared from different microwaving time and concentration of silver carbamate in AMP solution.

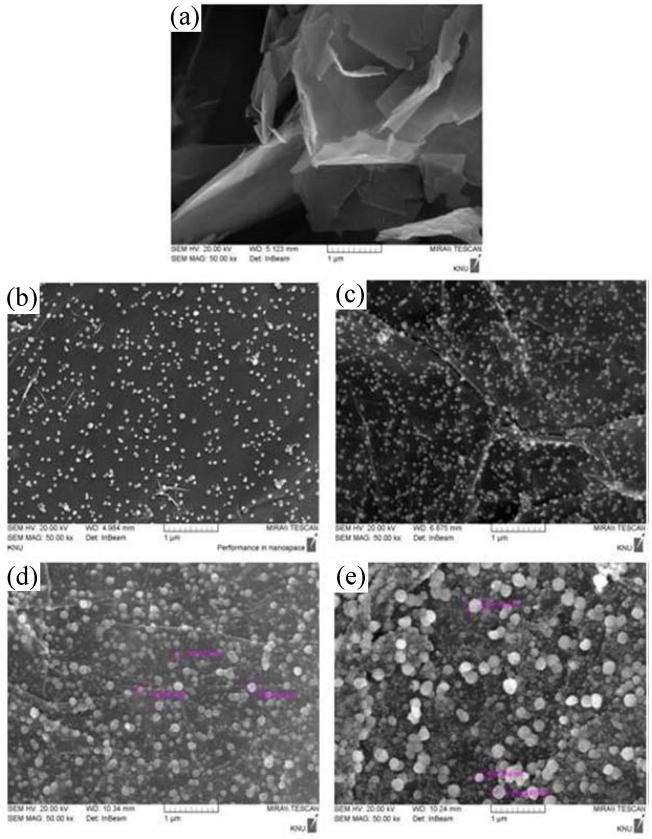

Figure 2. SEM images of (a) graphene, (b) S1, (c) S5, (d) S6 and (e) S8 prepared from different concentration of silver carbamate in AMP solution.

UV Spectra Analysis. As shown in the UV-vis spectra of Figure 3, when microwave time was extended to 3, 7, and 13 s, the specific absorption that occurred at 292 nm, which corresponded to the π-π* transitions of aromatic C–C bonds for graphene, was shifted to 426 nm. The surface plasmon

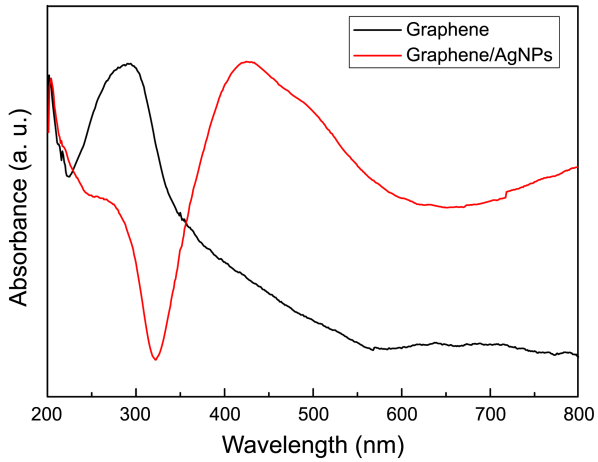

Figure 3. UV-vis absorption spectra of (a) graphene and (b) graphene/AgNPs composites obtained from Ag carbamate using irradiation of microwave for 13 seconds.

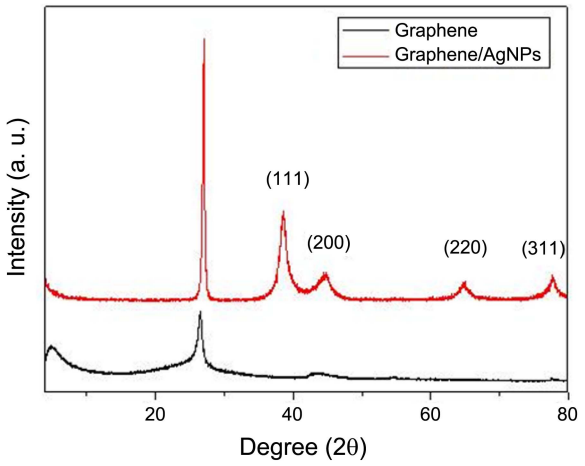

Figure 4. XRD patterns of graphene and graphene/AgNPs.

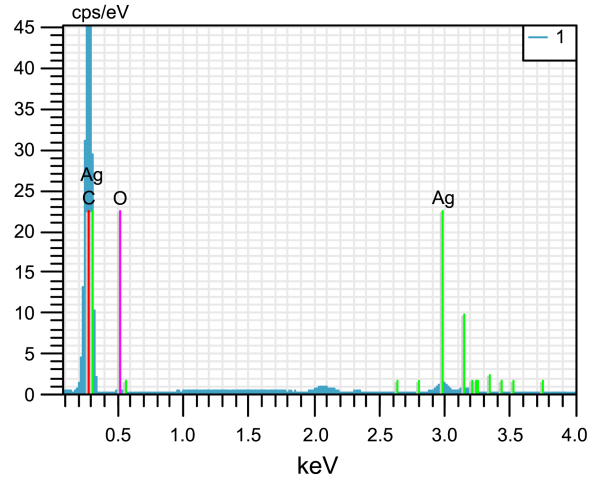

Figure 5. EDS analysis pattern of graphene/AgNPs.

band of AgNPs in the graphene/Ag heterostructures was red-shifted to 426 nm, which was mainly due to the change in the dielectric environment and the electron density of the AgNPs induced by the graphite sheets.[20] Its intensity and full width at half maximum were very large. The Mie theory states that narrow, symmetric peaks are expected from monodispersed solution systems and that polydispersed systems should show asymmetric peaks, suggesting the presence of two or more overlapping absorption peaks.[21,22] Therefore these results show that the AgNPs were irregular, corroborating the TEM images in Figure 1.

XRD and Energy Dispersive X-ray Spectroscopy (EDS) Analysis. The XRD patterns of the graphene and graphene/AgNPs are shown in Figure 4. These results show that graphene exhibited a characteristic peak (002) of graphene at 26.4°, which indicated the high crystallinity as shown in pristine graphite (JCPDS No. 41-1487). Four main peaks were observed in the XRD pattern of the graphene/AgNPs (Figure 4) at 2θ = 38.2°, 44.4°, 64.5° and 77.5°, which corresponded to the (111), (200), (220) and (311) planes of the cubic Ag crystal (JCPDS No. 04-0783), respectively, indicating that the metallic AgNPs were formed after reduction. It was also observed that the d-spacing value of the synthesized AgNPs using different dosages of silver carbamate remained almost constant for each crystallographic plane.

The graphene/AgNPs sample had 91.97 C wt % and Ag 4.76 wt %, and 96.63 C atom% and 0.52 Ag atom% content by the EDS analysis, as shown in Figure 5. Higher silver content was observed for the samples using a high concentration of silver carbamate, indicating that silver was effectively formed by the microwaving reduction of silver carbamate in the AMP medium.

FT-IR Spectra Analysis. The FT-IR spectra of GO, graphene and graphene/AgNPs are shown in Figure 6. The peaks at 1626, 1245 and 1060 cm^{-1} of GO (Figure 6(a)) are assigned to C=O stretching of COOH groups, skeletal vibrations of unoxidized graphitic domains, epoxy symmetrical ring deformation vibrations and C-O stretching vibrations, respectively, were removed completely (Figure 6(b)).[19,22,23] These FT-IR results demonstrate that GO was successfully reduced

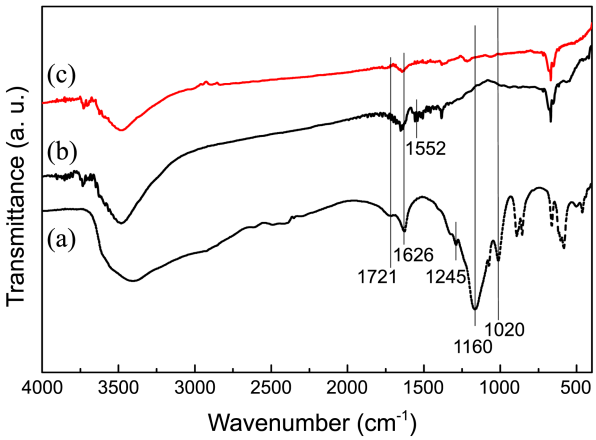

Figure 6. FTIR spectra of samples (a) GO, (b) graphene and (c) graphene/AgNPs.

to graphene. The new absorption band at 1552 cm^{-1} of graphene was attributed to the skeletal vibration of the graphene sheets.[21,22] The strong interactions may exist between AgNPs and graphene through π-interaction, but the absorption bands were quite week because of shield effect of AgNPs (Figure 6(c)).

Raman Spectral Analysis. Raman spectroscopy is a powerful nondestructive tool to characterize carbonaceous materials, particularly for distinguishing ordered and disordered carbon structures. As seen in Figure 7, the Raman spectrum of graphene displayed two prominent peaks at 1332 cm^{-1} (D band) and at 1562 cm^{-1} (G band), which are usually assigned to the breathing mode of point phonons of A_{1g} symmetry and the E_{2g} phonon of Csp2 atoms, respectively.[22,23] The Raman spectrum of graphene/AgNPs shows a G band at 1586 cm^{-1} and a D band at 1330 cm^{-1}. The ratio of the intensities of the D and G bands (ID/IG) decreased from 0.99 to 0.97, which was attributed to the increase in the mean crystallite size of graphene/AgNPs relative to that of graphene after loading AgNPs on graphene. The ID/IG ratio is inversely proportional to the reciprocal of the average crystallite size in graphite materials.[24] In addition, the peak

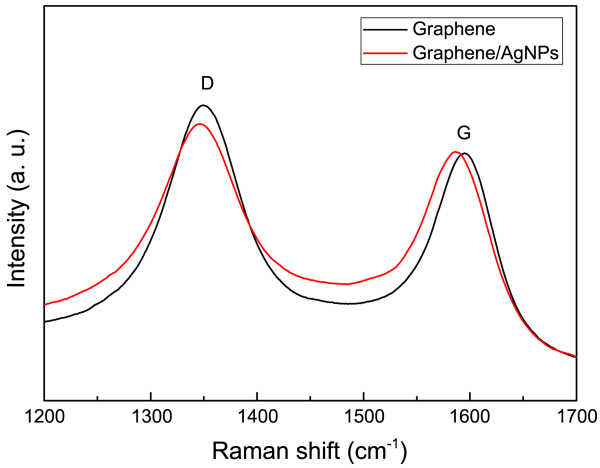

Figure 7. Raman spectra of (a) graphene and (b) graphene/AgNPs.

intensities of the D and G bands in graphene/AgNPs increased significantly in comparison with graphene. This result indicates that the surface-enhanced Raman scattering activity was due to the intense local electromagnetic fields of the AgNPs.[25]

Optical/Electrical Properties. Figure 8 displays an optical image of these films mounted on a transparent plastic sheet, which was positioned above a DKU logo to illustrate the level of optical transparency. Solution-based graphene layers usually produce multilayered graphene, but it is advantageous in terms of simple coating for transparent conductive films. The good anti-reflectance property of AgNPs might be expected for high transmittance. However, the corresponding transmittances at 550 nm for the as deposited graphene (68.3%), graphene/Ag (62.5%), and graphene/AgNPs (55.4%) are shown in Figure 9. Ag-decorated graphene lead to a decrease in the transparency of thin films that was lower than that for graphene. The optical properties of

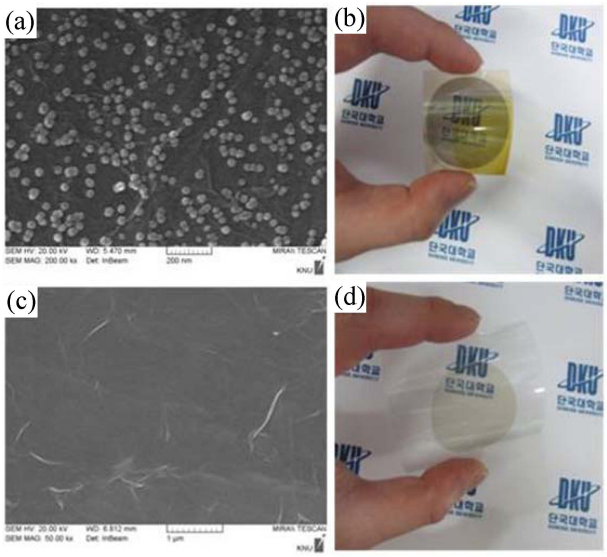

Figure 8. SEM image of coating surface of (a) graphene/AgNPs and (c) graphene, and optical image of (b) graphene/AgNPs and (d) graphene coating mounted on a PET film.

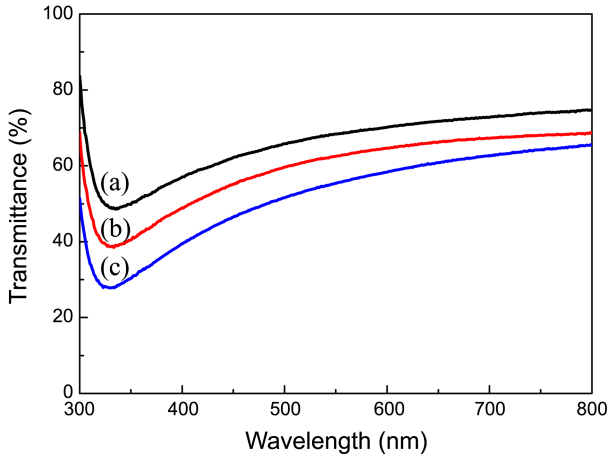

Figure 9. Transparency of the films obtained from (a) graphene, (b) graphene dispersed in silver carbamate and (c) graphene/AgNPs.

AgNPs are highly dependent on their size and shape. Due to the excitation of higher-order mode, large NPs have scatter predominantly in the forward direction (which is crucial for reducing surface reflectance).[26] Importantly, the fraction of light scattered into the substrate depends greatly on the three-dimensional shape of the AgNPs.[27] AgNPs with relatively big size (> 80 nm) and hemisphere morphology will make contributions to the good anti-reflection property. Thus, AgNPs decorated on the graphene film with proper size and islanding hemisphere morphology reduced the surface reflectance of the film through scattering the light onto the film.

The graphene/AgNPs yielded thin films with properties resembling those of graphene. More interestingly, by controlling the amount of AgNPs on the surface, it was possible to tune the electronic properties of the thin films.

The surface resistivity of the graphene or graphene/AgNPs-coated film was investigated. Figure 10 shows that the sheet resistance of the graphene film was 42.43 kΩ/□ at room

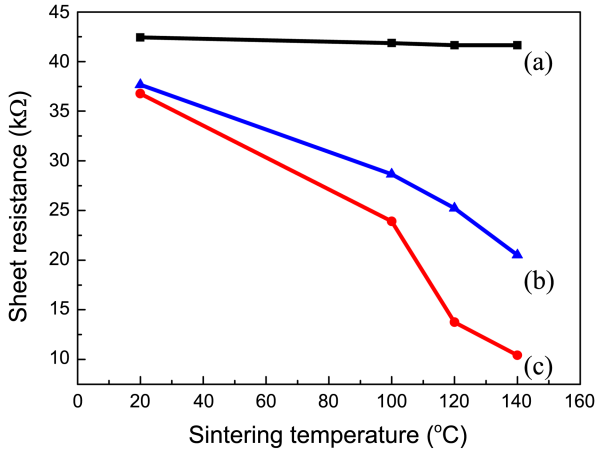

Figure 10. Sheet resistance of the transparent films obtained from (a) graphene, (b) graphene/AgNPs and (c) graphene dispersed in silver carbamate.

temperature, whereas the graphene/AgNPs films exhibited 37.66 kΩ/□ (Figure 10). However, annealing up to 140 °C under vacuum lead to a dramatic reduction in the sheet resistance. The lowest sheet resistance value of graphene/AgNPs obtained was 20.55 kΩ/□. The reason for the graphene film with a relatively high surface resistance is that the number of graphene sheets carbonized into small sheets, which cause restacking and holes on the surfaces of graphene film, decreased the number of electron transmission paths. For the comparison of conductivity and transparency of graphene and graphene/AgNPs, graphene/Ag film was prepared from graphene dispersed in silver carbamate solution. However, two factors cause the conductive behavior of a graphene/Ag film to be more optimal than that of a graphene film. First, incorporating AgNPs between graphene sheets hinders restacking and provides conductive paths between sheets. Second, the graphene/AgNPs film was flatter than that of the graphene film and had few defects, resulting in continuous electron transmission in graphene/AgNPs films. The conductivity will not improve simply by increasing the concentration of AgNPs.[28]

Conclusion

We report here an easy method to prepare graphene/AgNPs using microwave in AMP as a weak reducing agent. Uniform AgNPs with sizes of 20–200 nm were effectively decorated onto the grapheme surface while microwaving a silver carbamate complex in AMP for 3–13 seconds. The synthetic methods were simple and effective, allowing AgNPs to be uniformly anchored on the surfaces of reduced graphene nanosheets. This method can be potentially used as a tool to prepare graphene/AgNPs to enable control of particle size in the nanometer scale as well as the uniformity of particle size.

Acknowledgments. This work is supported by Grants from Priority Research Centers Program (2009-0093829).

References

1. Geim, A. K.; Novoselov, K. S. *Nat. Mater*. **2007**, *6*, 183.
2. Balandin, A. A.; Ghosh, S.; Bao, W.; Calizo, I.; Teweldebrhan, D.; Miao, F.; Lau, C. N. *Nano Lett*. **2008**, *8*, 902.
3. Li, D.; Muller, M. B.; Gijie, S.; Kaner, R. B.; Wallace, G. G. *Nat. Nanotechnol*. **2008**, *3*, 101.
4. Hu, W. B.; Peng, C.; Luo, W. J.; Lv, M.; Li, X. M.; Li, D.; Huang, Q.; Fan, C. H. *ACS Nano* **2010**, *4*, 4317.
5. Li, D.; Kaner, R. B. *Science* **2008**, *320*, 1170.
6. Stankovich, S.; Piner, R. D.; Chen, X. Q.; Wu, N. Q.; Nguyen, S. T.; Ruoff, R. S. *J. Mater. Chem*. **2006**, *16*, 155.
7. Xu, C.; Wu, X. D.; Zhu, J. W.; Wang, X. *Carbon* **2008**, *46*, 386.
8. Chen, J. L.; Yan, X. P. *J. Mater. Chem*. **2010**, *20*, 4328.
9. Wang, G. X.; Wang, B.; Park, J.; Yang, J.; Shen, X. P.; Yao, J. *Carbon* **2009**, *47*, 68.
10. Eda, G.; Fanchini, G.; Chhowalla, M. *Nat. Nanotechnol*. **2008**, *3*, 270.
11. Yuge, R.; Zhang, M.; Tomonari, M.; Yoshitake, T.; Iijima, S.; Yudasaka, M. *ACS Nano* **2008**, *2*, 1865.
12. Shen, J. F.; Shi, M.; Li, N.; Yan, B.; Ma, H. W.; Hu, Y. Z.; Ye, M. X. *Nano Res*. **2010**, *3*, 339.
13. Chen, S.; Zhu, J. W.; Wang, X. *J. Phys. Chem. C* **2010**, *114*, 11829.
14. Zou, W. B.; Zhu, J. W.; Sun, Y. X.; Wang, X. *Mater. Chem. Phys*. **2011**, *125*, 617.
15. Chen, S.; Zhu, J. W.; Wu, W. D.; Han, Q. F.; Wang, X. *ACS Nano* **2010**, *4*, 2822.
16. Hummers, W. S.; Offeman, R. E. *J. Am. Chem. Soc.* **1958**, *80*, 1339.
17. Stankovich, S.; Dikin, D. A.; Piner, R. D.; Kohlhaas, K. A.; Kleinhammes, A.; Jia, Y.; Wu, Y.; Nguyen, S. T.; Ruoff, R. S. *Carbon* **2007**, *45*, 1558.
18. Park, H. S.; Shin, U. S.; Kim, H. W.; Gong, M. S. *Bull. Korean Chem. Soc*. **2011**, *32*, 273.
19. Park, H. S.; Gong, M. S. *Bull. Korean Chem. Soc*. **2012**, *33*, 483.
20. Mulvaney, P. *Langmuir* **1996**, *12*, 788.
21. Bhui, D. K.; Bar, H.; Sarkar, P.; Sahoo, G. P.; De, S. P.; Misra, A. *J. Mol. Liquids* **2009**, *145*, 33.
22. Nguyena, V. H.; Kim, B. K.; Jo, Y. L.; Shim, J. J. *J. Supercritical Fluids* **2012**, *72*, 28.
23. Zainy, M.; Huang, N. M.; VijayKumar, S.; Lim, H. N.; Chia, C. H.; Harrison, I. *Mater. Lett*. **2012**, *89*, 180.
24. Pimenta, M. A.; Dresselhaus, G.; Dresselhaus, M. S.; Cancado, L. G.; Jorio, A.; Saito, R. *Phys. Chem. Chem. Phys*. **2007**, *9*, 1276.
25. Li, J.; Liu, C. *Eur. J. Inorg. Chem*. **2010**, 1244.
26. Temple, T. L.; Mahanama, G. D. K.; Reehal, H. S.; Bagnall, D. M. *Sol. Energy Mater. Sol. Cells* **2009**, *93*, 1978.
27. Catchpole, K. R.; Polman, A. *Appl. Phys. Lett*. **2008**, *93*, 1911131.
28. Zhou, Y.; Yang, J.; Cheng, X.; Zhao, N.; Sun, L.; Sun, H.; Li, D. *Carbon* **2012**, *50*, 4343.